Supporting Information

Morphology-Controlled Monolithic $SrTiO_3$/Ti Nanocatalysts with Dispersed Rh Single Atoms and Clusters for Highly Selective Photocatalytic CO_2 Reduction to CH_4

Mingjun Liu[a,b], Wenduo Yang[a,b], Jinrui Gao[a,b], Tongxiang Chen[a,b], Haijin Zhang[a,b], *Renat Beissenov,*[c] Zhaolin Na [a,b], Jing Li [a,b,*] and Baodan Liu [a,b,*]

[a] School of Materials Science and Engineering, Northeastern University, No.11, Wenhua Road, Shenyang, 110819, China

[b] Foshan Graduate School of Innovation, Northeastern University, No. 2, Zhihui Road, Shunde District, Foshan, 528300, China

[c] Kazakh-British Technical University, Tole Bi Street 59, Almaty, 050000, Kazakhstan

* Corresponding Author: lijing1@mail.neu.edu.cn; baodanliu@hotmail.com

Figures

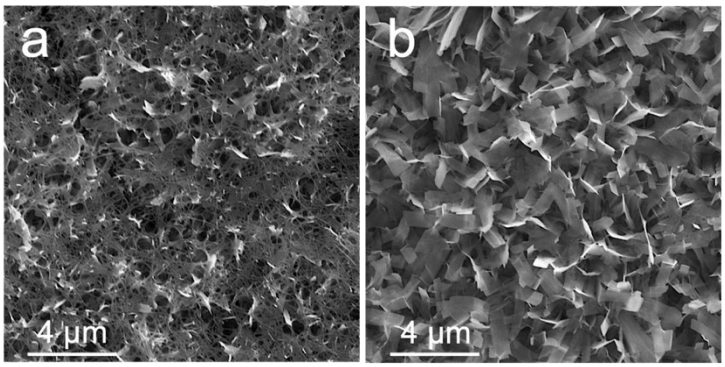

Fig. S1. SEM images of the $Na_2Ti_2O_5$ precursors for $SrTiO_3$ samples with different morphologies: (a) nanowires; (b)nanosheets.

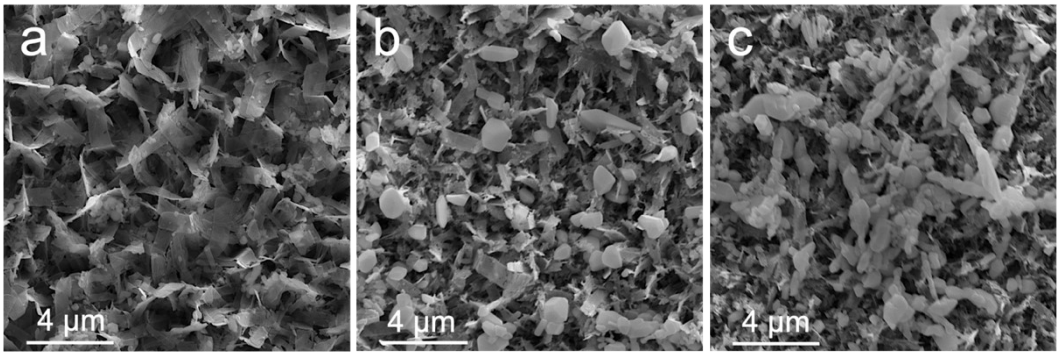

Fig. S2. SEM images of $SrTiO_3$/Ti samples obtained with different secondary hydrothermal reaction times: (a) 2 h; (b) 4 h; (c) 8 h.

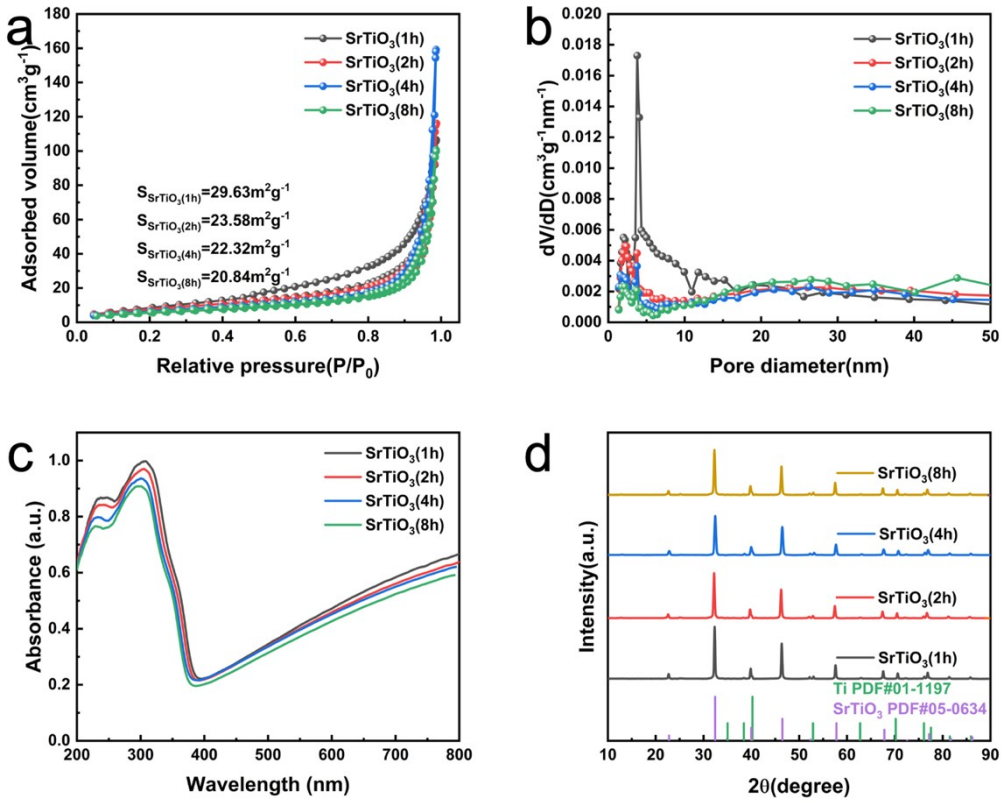

Fig. S3. Structural and optical characterization of $SrTiO_3$/Ti samples prepared with different secondary hydrothermal durations (1, 2, 4, and 8 h): (a) N_2 adsorption–desorption isotherms; (b) pore size distribution curves; (c) UV–vis diffuse reflectance spectra; (d) XRD patterns.

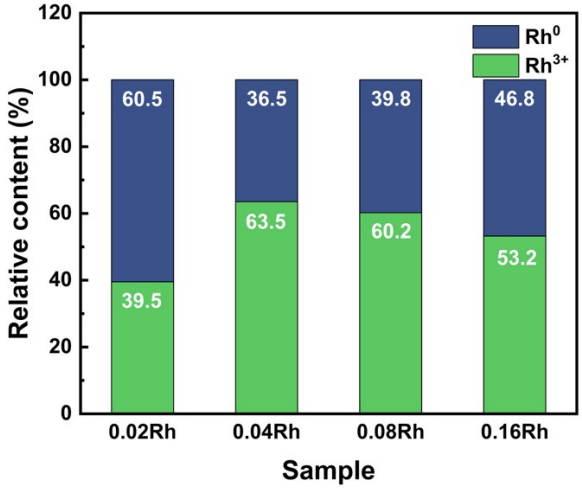

Fig. S4. Relative atomic contents of Rh^{3+} and Rh^0 in xRh/$SrTiO_3$/Ti samples with different Rh loadings.

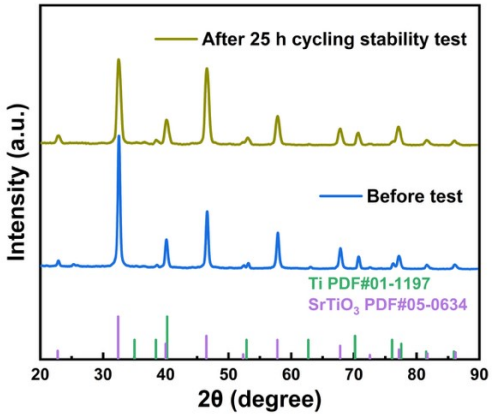

Fig. S5. XRD pattern of the 0.04Rh/$SrTiO_3$/Ti sample before test and after 25 h cycling stability test.

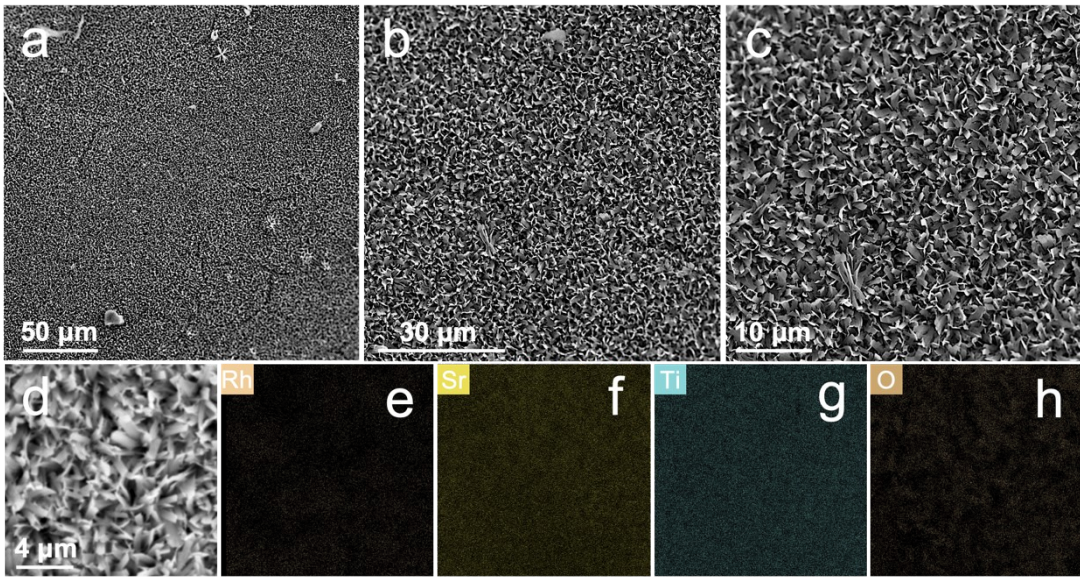

Fig. S6. SEM images and EDS elemental mapping images of 0.04Rh/$SrTiO_3$/Ti after 25 h of photocatalytic cycling stability test: (a-c) SEM images and (d-h) EDS elemental mappings.

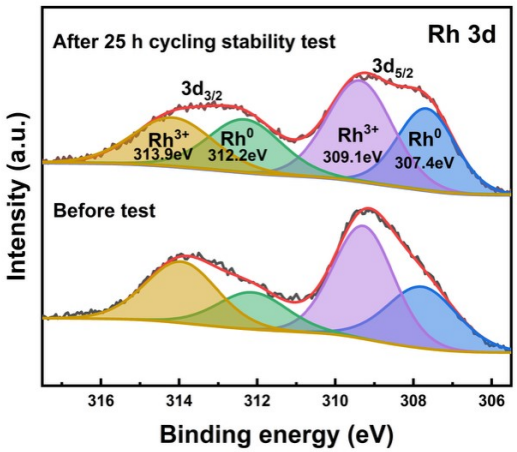

Fig. S7. XPS spectra of the 0.04Rh/$SrTiO_3$/Ti sample before test and after 25 h of cycling stability test.

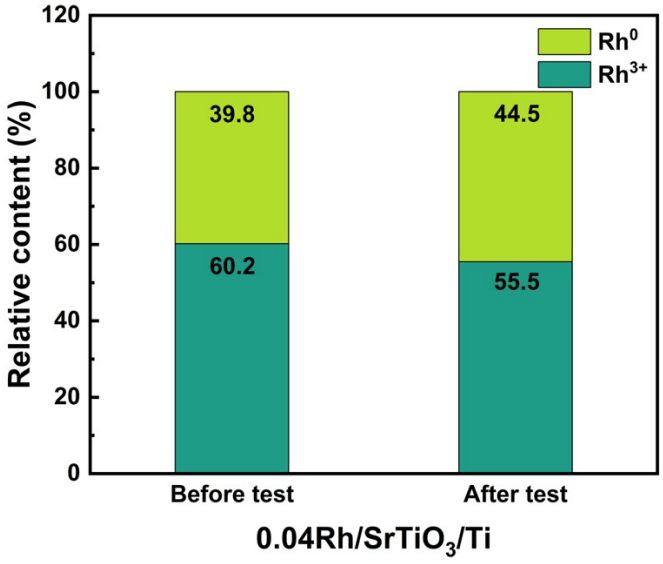

Fig. S8. Relative atomic contents of Rh^{3+} and Rh^{0} of the $0.04Rh/SrTiO_3/Ti$ sample before test and after 25 h of cycling stability test.

Table S1. Elemental contents of Rh, Sr and Ti in 0.04Rh/$SrTiO_3$/Ti sample determined by ICP-MS.

Element	Rh	Sr	Ti
Content (wt.%)	0.0941	40.3386	24.2597

Table S2. Comparison of CH_4 production rates and selectivity for CO_2 photoreduction over $SrTiO_3$-based photocatalysts and previously reported catalysts in recent years.

Catalysts	Reaction conditions	Light sources	CH_4 Yield ($\mu mol \cdot g^{-1} \cdot h^{-1}$)	CH_4 Selectivity (%)	refs
$Pt/SrTiO_3$	CO_2 gas (1 atm) and 0.4 mL H_2O, >125 °C	300 W Xe-lamp	1.61	100	[1]
$C/TiO_2/SrTiO_3$	CO_2 gas (100 kPa) and 150 mL H_2O,5°C	300 W Xe-lamp and a 3 a.m. 1.5 G filter	35.9	39.54	[2]
$Bi\text{-}SrTiO_{3-x}$	5 mg photocatalysts, CO_2 gas (0.1MPa) and 2 mL H_2O	300 W Xe-lamp ($\lambda >$ 420 nm) 200 $mW \cdot cm^{-2}$	0.36	6.06	[3]
$SnS_2/3DOM\text{-}SrTiO_3$	CO_2 gas and 2 mL H_2O	300 W Xe-lamp ($\lambda >$ 420 nm), 80 $mW \cdot cm^{-2}$	12.5	74.9	[4]
$Al/N\text{-}SrTiO_3$	CO_2 gas 50mL and 2mL H_2O,55°C	300 W Xe-lamp	0.81	13.43	[5]
$Bi_2SiO_5/SrTiO_3$	50 mg photocatalysts, high-purity CO_2 gas and saturated H_2O steam	300 W Xe-lamp	6.58	13.43	[6]
$TiO_2/SrTiO_3$	5 mg photocatalysts, CO_2 gas (1 atm) and 10 mL H_2O,30°C	300 W Xe-lamp ($320<\lambda<780$ nm)	0.65	1.91	[7]
$Pt/Cu/TiO_2$	20 mg photocatalysts, CO_2 and H_2O vapor	300 W Xe-lamp(300 nm < $\lambda<$ 400 nm)	2.5	100	[8]
$Sr_{0.8}Bi_{0.2}Ti_{0.8}Mn_{0.2}O_3$	20 mg photocatalysts, CO_2 gas (1.5 atm) and 2 mL H_2O,75°C	300 W Xe-lamp 200 $mW \cdot cm^{-2}$	30.6	84.3	[9]
$TiO_2\text{-}V_{TI}\text{-}V_O$	10 mg photocatalysts, pure	300 W Xe-lamp	19.4	100	[10]

Catalysts	Reaction conditions	Light sources	CH_4 Yield ($\mu mol \cdot g^{-1} \cdot h^{-1}$)	CH_4 Selectivity (%)	refs
g-C_3N_4/ La-Rh-$SrTiO_3$	CO_2 with H_2O vapor(101 kPa), 20°C 50 mg photocatalysts, pure CO_2 with H_2O vapor	300 W Xe-lamp	1.8	30.51	[11]
Rh/$SrTiO_3$/Ti	CO_2 gas (80 kPa) and 1mL H_2O, 30°C	300 W Xe-lamp	35.62	100	This work

References

1. L. Lu, X. He, X. Zhu, C. Lv, Z. Liu, L. Pei, S. Yan and Z. Zou, Inorg Chem, 2024, 63, 13295-13303.
2. Q. S. Wang, Y. C. Yuan, C. F. Li, Z.-r. Zhang, C. Xia, W.-g. Pan, L. Liu and R.-t. Guo, Renewable Energy, 2024, 231, 120997.
3. L. Pan, H. Mei, G. Zhu, S. Li, X. Xie, S. Gong, H. Liu, Z. Jin, J. Gao, L. Cheng and L. Zhang, Journal of Colloid and Interface Science, 2022, 611, 137-148.
4. W. He, X. Wu, Y. Li, J. Xiong, Z. Tang, Y. Wei, Z. Zhao, X. Zhang and J. Liu, Chinese Chemical Letters, 2020, 31, 2774-2778.
5. W. Wang, W. Kang, J. Niu, H. Jian, Q. Shen and J. Xue, J Colloid Interface Sci, 2025, 689, 137266.
6. T. T. Han, Y. Guo, M. A. Mushtaq and Y. Jia, J Environ Chem Eng, 2025, 13, 117604.
7. S. Jiang, K. Zhao, M. Al Mamun, Y. L. Zhong, P. Liu, H. Yin, L. Jiang, S. Lowe, J. Qi and R. Yu, Inorg Chem Front, 2019, 6, 1667-1674.
8. J. Wang, Y. Li, J. Zhao, Z. Xiong, Y. Zhao and J. Zhang, Catalysis Science & Technology, 2022, 12, 3454-3463.
9. Y. Gao, M. Zhang, Y. Jin, Y. Mao, W. Wang and Z. Song, ACS Catalysis, 2024, 14, 10746-10759.
10. Y. He, S. Dai, J. P. Sheng, Q. Ren, Y. Lv, Y. Sun and F. Dong, Proceedings of the National Academy of Sciences, 2024, 121, e2322107121.
11. S. J. Wan, Y. T. Hou, W. Wang, G. Q. Luo, C.-B. Wang, R. Tu and S.-W. Cao, Rare Met, 2024, 43, 5880-5890.